
Bifunctional Effects of Lactoferrin (LFcinB11) in Inhibiting Neural Cell Adhesive Molecule (NCAM) Polysialylation and Neutrophil Extracellular Traps (NET) Release

Bo Lu , Si-Ming Liao , Shi-Jie Liang , Li-Xin Peng , [Jian-Xiu Li](#) , Xue-Hui Liu , [Ri-Bo Huang](#) ^{*} , [Guo-Ping Zhou](#) ^{*}

Posted Date: 26 March 2024

doi: 10.20944/preprints202403.1534.v1

Keywords: polysialic acid; polysialyltransferase; polysialyltransferase domain; chemical shift perturbation; NMR spectroscopy; Lactoferrin



Preprints.org is a free multidiscipline platform providing preprint service that is dedicated to making early versions of research outputs permanently available and citable. Preprints posted at Preprints.org appear in Web of Science, Crossref, Google Scholar, Scilit, Europe PMC.

Copyright: This is an open access article distributed under the Creative Commons Attribution License which permits unrestricted use, distribution, and reproduction in any medium, provided the original work is properly cited.

Article

Bifunctional Effects of Lactoferrin (LFcinB11) in Inhibiting Neural Cell Adhesive Molecule (NCAM) Polysialylation and Neutrophil Extracellular Traps (NET) Release

Bo Lu ^{1,†}, Si-Ming Liao ^{1,†}, Shi-Jie Liang ¹, Li-Xin Peng ¹, Jian-Xiu Li ¹, Xue-Hui Liu ²,
Ri-Bo Huang ^{1,3,4,*} and Guo-Ping Zhou ^{1,4,*}

¹ National Engineering Research Center for Non-food Biorefinery, Guangxi Academy of Sciences, 98 Daling Road, Nanning, Guangxi 530007, China

² Institute of Biophysics, Chinese Academy of Sciences, Beijing, P.R. China

³ Life Science and Technology College, Guangxi University, Nanning, Guangxi, 530004 China

⁴ Rocky Mount Life Science Institute, NC, USA

* Correspondence: rbhuang@gxas.cn (R.-B.H.); gpzhou@rmlsi.ac (G.-P.Z.)

† Authors contributed equally.

Abstract: The expression of polysialic acid (polySia) on the neuronal cell adhesion molecule (NCAM), is called NCAM-polysialylation, which is strongly related to the migration and invasion of tumor cells and with aggressive in the clinic. Thus, it's important to select a proper drug to block tumor cell migration for clinic treatment. In this study, we proposed that lactoferrin (LFcinB11) may be a more ideal candidate for inhibition of NCAM polysialylation comparing with CMP and low molecular weight heparin (LMWH), which were determined based on our NMR studies. On the other hand, because neutrophil extracellular traps (NET) is the most dramatic stage in cell death process, and NETs' release are related to pathogenesis of autoimmune and inflammatory disorders, with proposed involvement in glomerulonephritis, chronic lung disease, sepsis and vascular disorders. In this study, the molecular mechanism of inhibition of NETs' release using LFcinB11 as inhibitor was also determined. Based on these results, LFcinB11 is proposed to be bifunctional inhibitor for inhibiting both NCAM polysialylation and NETs releases.

Keywords: polysialic acid; polysialyltransferase; polysialyltransferase domain; chemical shift perturbation; NMR spectroscopy; lactoferrin

1. Introduction

Polysialic acid (polySia) expression on neuronal cell adhesion molecule (NCAM) [1–7] is called NCAM polysialylation, which is related to cancer cell migration through the interactions between polysialyltransferases (polySTs) and CMP-Sia, and polyST and polysialic acid (polySia) [8,9]. More specifically, these interactions are actually the direct bindings of Polysialyltransferase Domain (PSTD) to CMP-Sia, and PSTD to polySia [10–15]. PSTD is a polybasic motif of 32 amino acids in two polySTs, ST8SiaIV and ST8SiaII [16].

Inhibition of posttranslational modifications (PTM) is related to a number of diseases such as cancer, nervous and cardiovascular system diseases. One of the latest advances in PTM research is inhibition of polysialylation of neuronal cell adhesion molecule (NCAM) [17,18], which is strongly related to the migration and invasion of tumor cells and with aggressive, metastatic disease and poor clinical prognosis in the clinic due to the formation of polysialic acid (poly-Sia) on the surface of NCAM [19–22].

It has been known that NCAM-polySia expression on cancer cells is catalyzed by two polysialyltransferases (polySTs), ST8SiaIV and ST8SiaII, and specifically two polybasic motifs, Polybasic Region (PBR) and Polysialyltransferase Domain (PSTD) within each polyST, have been

found to be critically important for polyST activity based on recent mutation and molecular modeling analyses [16,23]. Thus, the intermolecular interactions of PBR-NCAM, PSTD-polySia and PSTD-(CMP-sialic acid) have been suggested during NCAM polysialylation and tested by more recent NMR studies [14]. Furthermore, a modulation model of NCAM-polysialylation and cell migration has been proposed by incorporating the intramolecular interaction of PBR-PSTD into above intermolecular interaction [14]. This model has been further supported using Chou's wenxiang diagram method [24–28].

Two inhibitors of NCAM polysialylation, Low-molecular-weight *heparin* (LMWH) and cytidine monophosphate (CMP), have been proposed as drug research and help to development related to the tumor-targeted polysialyltransferases based on above modulation model of NCAM-polysialylation.

The previous in vitro study showed that heparin LMWH is an efficient inhibitor due to its stronger binding to the PSTD [16], and was further supported using the recent NMR studies [23]. However, the use of heparin should be carefully, because the previous reports indicated that intracerebral hemorrhage of patients were related to heparin intake [29].

Another inhibitor, cytidine monophosphate (CMP) has been also verified that the polysialylation could be partially inhibited when CMP-Sia and polySia co-exist in solution by the recent NMR studies. CMP-Sia may play a role in reducing the gathering extent of polySia chains on the PSTD, and may benefit for the inhibition of polysialylation [30]. However, CMP could not inhibit the PSTD-polySia interaction [30].

Lactoferrin (LF) is an iron-binding glycoprotein composed of 49 amino acids, and has antimicrobial, antiviral, antitumor, and immunological activity [31]. In the more recent studies, a 11-residual peptide (RRWQWRMCKKLG) from the N-terminus [32] of LF, was designed as (LFcinB11), which has also similar antimicrobial activities in bovine lactoferricin (BLFC) [33,34].

In this study, our interest is to determine whether can LFcinB11 also inhibit NCAM polysialylation? If so, what its minimum concentration to ensure its inhibitory effect on the polysialylation?

In addition, the previous study has proposed that the release of neutrophil extracellular traps (NET) could be inhibited through the interaction between polySia and LF, using a native gel electrophoresis application using in vitro experiments [31–33]. In the current study, molecular mechanism of this interaction is determined based on our NMR studies. Thus, LFcinB11 may play a bifunctional role in inhibition of formation of NETs and NCAM polysialylation.

2. Results

2.1. CD Data

As shown in Figure 1, our CD spectra display that the α -helical content of the PSTD contains 23.0% in the absence of any ligands. The helical contents were decreased to 16.4% after adding the mixture of 40 μ M (CMP-Sia) and 4 μ M polySia, and was further decreased to 14.8% after added LFcinB11. These results suggested the helices in the PSTD were unwound due to the addition of the mixture of CMP-Sia and polySia, and further unwinding after adding LFcinB11. The decreases of helical contents in the PSTD indicate its conformational change and verified the PSTD not only interact with the mixture of CMP-Sia and polySia as the previous study [10–14], but also suggest an interaction between the PSTD and LFcinB11. However, the difference of 16.4% and 14.8% is only 1.6%. This means that the helical structure of the PSTD is basically stable after LFcinB11 was added to the sample. A possible explanation is that there is an interaction between LFcinB11 and polySia. Because This interaction may decrease the helical unwinding extent in the PSTD.

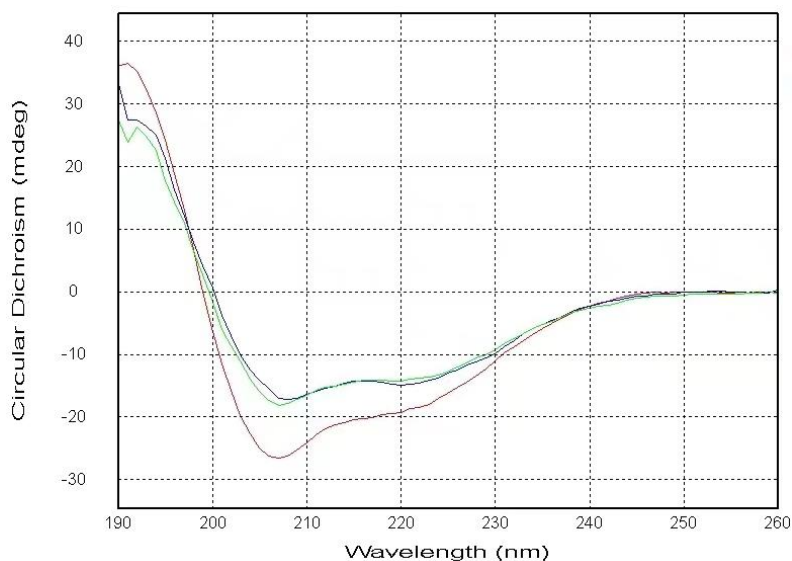


Figure 1. The CD spectra of the PSTD in the absence (red), and the presence of the mixture of CMP-Sia and polySia (green), and the mixture of CMP-Sia, polySia and LFcInB11 (blue). The helical contents of these three CD spectra of the PSTD are 23%, 16.4%, and 14.8%, respectively.

2.2. NMR Results (a)

In order to verify the interaction between the PSTD and LFcInB11, 2D-HSQC experiments of the mixtures of the LFcInB11 with different concentration and the PSTD were carried out. In addition, the PSTD-LFcInB11 interaction was also tested.

2.2.1. The Interaction between the PSTD and 20 μ M LFcInB11

In this study, the overlaid HSQC spectra of the PSTD for the PSTD-(20 μ M LFcInB11) interaction, showed that the significant changes in chemical shift are found in 8 residues, K246, K250, V251, R252, T253, S257, V273 and I275 (Table 1 & Figure 2A), in which most residues are located on the binding region of CMP-Sia (K246-L258) (Table 2) except from two residues V273 and I275 (Figure 2A). In addition, the CSP values in this range (K246-L258) for the PSTD-20 μ M LFcInB11 interaction are less than that for the PSTD-(CMP-Sia) interaction (Figure 2). These results indicate that 20 μ M LFcInB11 could not inhibit the interaction between the PSTD-(CMP-Sia). Similarly, the CSPs values in the polySia binding region of the PSTD (A263-N271) are also smaller than that for the PSTD-polySia interaction (Figure 3).

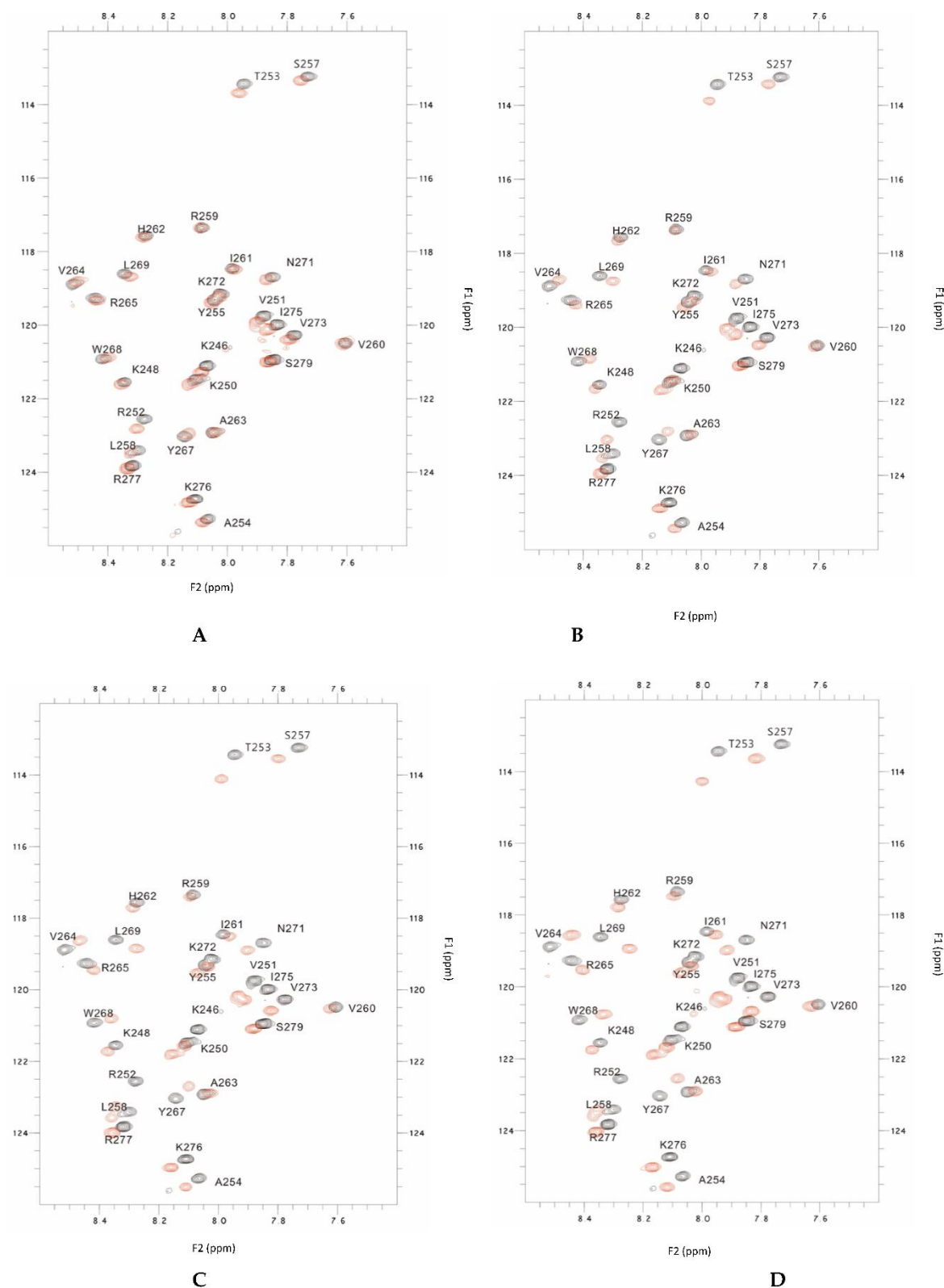
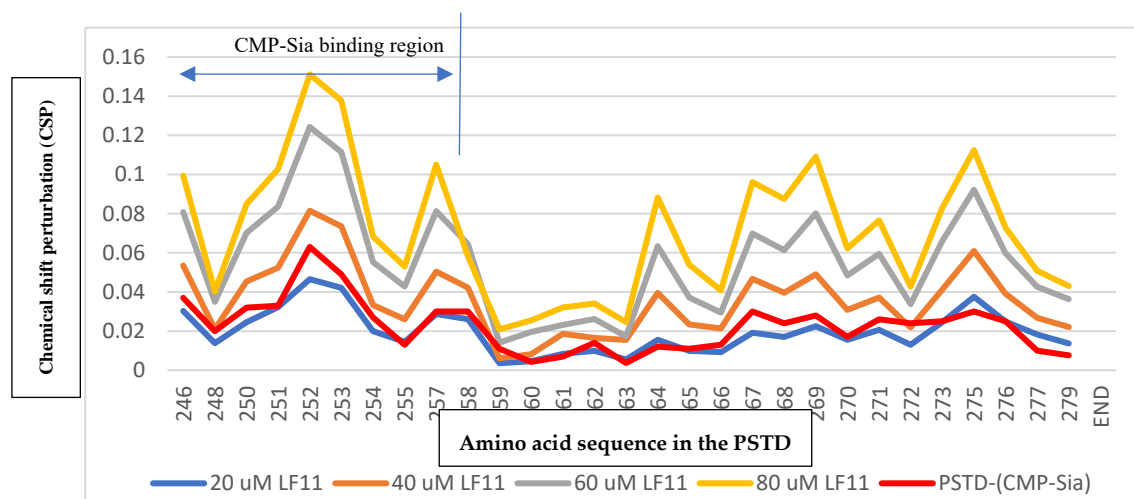
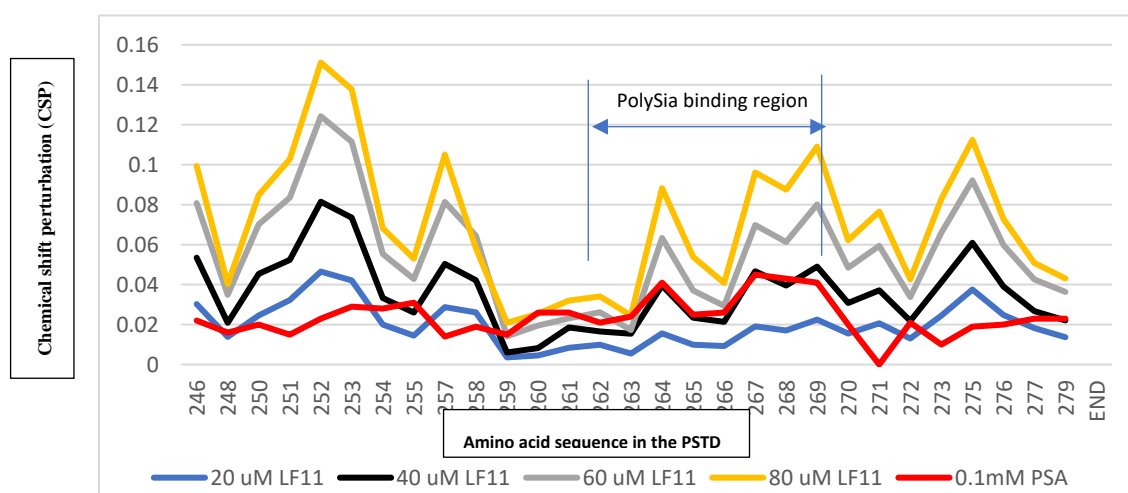


Figure 2. The overlaid ^1H - ^{15}N HSQC spectra of the 2mM PSTD in the absence and the presence of 20uM LFcInB11 (A), and 40uM LFcInB11 (B), and 60uM LFcInB11 (C) and 80uM LFcInB11, respectively.



(A)



(B)

Figure 3. Chemical shift perturbations (CSPs) of the PSTD when the PSTD interacted with 20uM LFcInB11 (blue), 40uM LFcInB11 (orange), 60uM LFcInB11 (gray), and 1mM CMP-Sia (red), respectively (A); Chemical shift perturbations (CSPs) of the PSTD when the PSTD interacted with 20uM LFcInB11 (blue), 40uM LFcInB11 (black), 60uM LFcInB11 (gray), 80uM LFcInB11 (orange), and 0.1mM polySia (red), respectively (B).

Table 1. The effect of different lactoferrin concentrations (20uM, 40uM, 60uM and 80uM) on chemical shift of the residues for the PSTD-LFcInB11 interaction based on the data from Figures 2 and 3.

LFcInB11 concentration interacted with the PSTD	Residues in the PSTD that do not change in chemical shift	Residues in the PSTD that changed in chemical shift
20 uM	17 residues (K248,A254,Y255,L258,R259,V260,I261,H262,A263,V264,R265,Y267,W268,L269,K272,K276,S279)	8 residues (K246,K250,V251,R252,T253,S257,V273,I275)
40 uM	6 residues (R259,V260,I261,H262,A263,K272)	19 residues (K246,K248,K250,V251,R252,T253,A254,Y255,S257,L258,V264,R265,Y267,W268,L269,V273,I275,R277,S279)
60 uM	3 residues (R259,V260,A263)	22 residues
80 uM	0 residues	25 residues

Table 2. The binding regions of CMP-Sia and polySia for the different ligands on the PSTD. The maximum CSPs in each binding region are compared with the maximum CSPs for the PSTD-(CMP-Sia) interaction and for the PSTD-polySia interaction, respectively. The all CSPs were obtained based on current and the previous 2D 1H-15N HSQC experiments [23,30].

Ligands binding to the PSTD	The maximum CSPs in CMP-Sia binding region (K246-L258)	The maximum CSPs in polySia binding region (A263-R271)
CMP-Sia	0.063	0.030
polySia	0.031	0.045
Heparin LMWH (80 uM)	0.087	0.072
CMP (1mM)	0.087	0.046
LFcinB11 (20 uM)	0.047	0.038
LFcinB11 (40 uM)	0.081	0.061
LFcinB11 (60 uM)	0.124	0.092
LFcinB11 (80 uM)	0.151	0.109

2.2.2. The Interaction between the PSTD and 40 uM LFcinB11

When LFcinB11 concentration was increased to 40 uM, the significant changes in chemical shift are found in 19 residues, K246, K248, K250, V251, R252, T253, A254, Y255, S257, L258, V264, R265, Y267, W268, L269, V273, I275, R277 and S279, and there are only 6 residues (R259, V260, I261, H262, A263 and K272) no change in chemical shift (Table 1 & Figure 2b). The CSPs for PSTD-40uM LFcinB11 interaction are larger than that for the PSTD-(CMP-Sia) and for the PSTD-20uM LFcinB11 interactions (Figure 3a) in the CMP-Sia binding region, indicating the PSTD-(CMP-Sia) interaction could be inhibited by 40uM LFcin. In addition, most CSPs for PSTD-40uM LFcin interaction and the PSTD-polySia interaction are very closed in the polySia binding region (Figure 3b). However, the CSPs for the former are larger than that for the later at residue L269 and N271 (Figure 3b). Thus suggest that the PSTD-polySia interaction could be inhibited when LFcinB11 concentration is more than 40uM.

2.2.3. The Interaction between the PSTD and 60 uM LFcinB11

LFcin11 concentration was increased to 60 uM, the significant changes in chemical shift are found in most residues according to the overlaid HSQC spectra (Figure 2C), and there are only 3 residues (R259, V260, and A263) no change in chemical shift (Table 1 & Figure 2C). The CSPs for PSTD-60uM LFcinB11 interaction are larger than that for the PSTD-(CMP-Sia) interaction (Figure 3a) in the CMP-Sia binding region, indicating the PSTD-(CMP-Sia) interaction could be inhibited by 60uM LFcinB11. In addition, the CSPs for PSTD-60uM LFcinB11 interaction are also larger than that for the PSTD-polySia interaction in the polySia binding region (Figure 3b), and thus further suggest that the PSTD-polySia interaction could be inhibited by 60uM LFcinB11.

2.2.4. The Interaction between the PSTD and 80 uM LFcinB11

When LFcinB11 concentration was increased to 80 uM, almost all residues of the PSTD have changed in chemical shift (Figure 2D), and the CSP of each residue is larger than that for the interaction between the PSTD and 60 uM LFcin. In the CMP-Sia binding region for the PSTD-(CMP-Sia) interaction, the maximum CSP is 0.151, which is larger than that for the PSTD-60uM LF, and in the polySia binding region, the maximum CSP is 0.109, which is also much larger than that for the PSTD-60uM LFcinB11 (Table 2). These results indicate that the CSPs in both CMP-Sia and polySia binding regions of the PSTD are increased with LF's concentration.

2.2.5. The Interaction between LFcinB11 and polySia

In order to determine the interaction between polySia and LFcinB11, the overlaid 2D 1H-15N HSQC spectra were carried out at our NMR spectrometer. As shown in Figure 4, there is no any

chemical shift is detected except residue 11G after polySia and LFcInB11 were mixed. However, the peak intensities of almost all residues were significantly decreased, thus suggesting the interaction between polySia and LFcInB11 through the formation of LFcInB11-polySia aggregates.

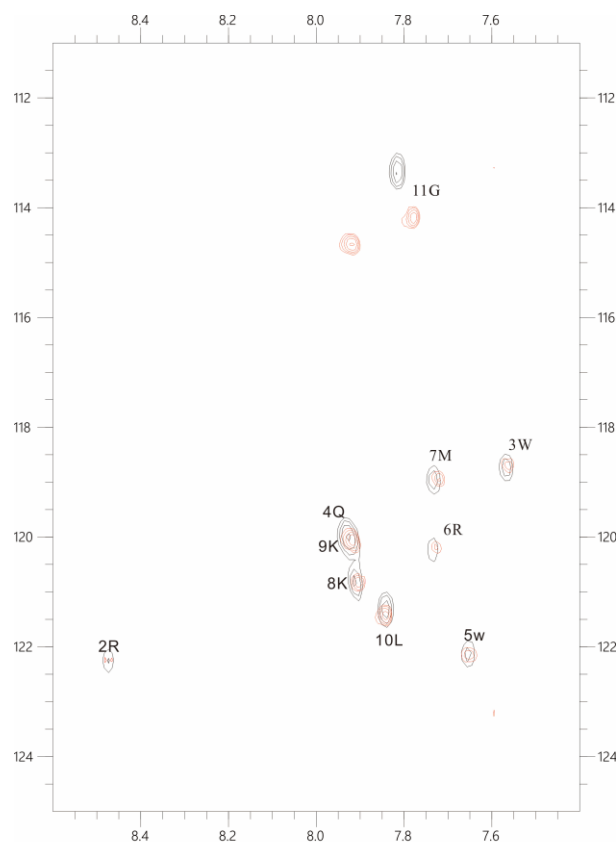


Figure 4. The overlaid ^1H - ^{15}N HSQC spectra of 50 μM LFcIn11 in the absence (black) and the presence of 50 μM polySia (red), respectively.

3. Discussion

So far both 3D X-ray and NMR structures of the polySTs have not yet been reported, due to the existence of many hydrophobic residues in the polySTs, which are in the membrane environment [13,14]. However, the 3-D solution structure of the PSTD peptide, an active site in the ST8Sia IV, has been obtained based on our NMR studies [10–14]. Thus, a hypothesis has been proposed: the interaction between the PSTD and the ligands such as CMP-Sia, polySia or any possible inhibitors may correspond to the interactions between the polyST and these ligands. This is an efficient research strategy and methodology for studying biological problems using biophysical and NMR structural biology. The above hypothesis has been successfully tested by the recent NMR studies [23–25].

Above CD spectra qualitatively demonstrate the possible interaction between the PSTD and LFcInB11. The more details of the interactions between the PSTD and LFcIn11 were provided by our NMR experimental results

The polysialylation of trimer of α -2,8-linked sialic acid (triSia) was inhibited by cytidine monophosphate (CMP) in the presence of ST8SiaII and CMP-Neu5Ac (CMP-Sia) based on in vitro experiments [30,35]. The more recent studies verified that the PSTD-(CMP-Sia) could be inhibited by CMP, but the PSTD-polySia binding could not be inhibited by CMP even in mixture status of CMP-Sia, polySia and the PSTD based on our NMR data [30].

There are two binding regions for CMP-Sia in the PSTD, one is in the residue range K246-L258, and other one in the range Y267-R277 [30]. The former is also the binding region of CMP, and the latter is covered in CMP-PSTD binding region (V264-K276) [30]. In this study, the CSP values for the

PSTD-LFcinB11 interactions are larger than that for the PSTD-CMP and the PSTD-polySia interactions when LFcinB11 concentration at least 40 μ M (Figure 5). These results indicate that LFcinB11 is more powerful in inhibiting both the PSTD-(CMP-Sia) and the PSTD-polySia interactions than CMP.

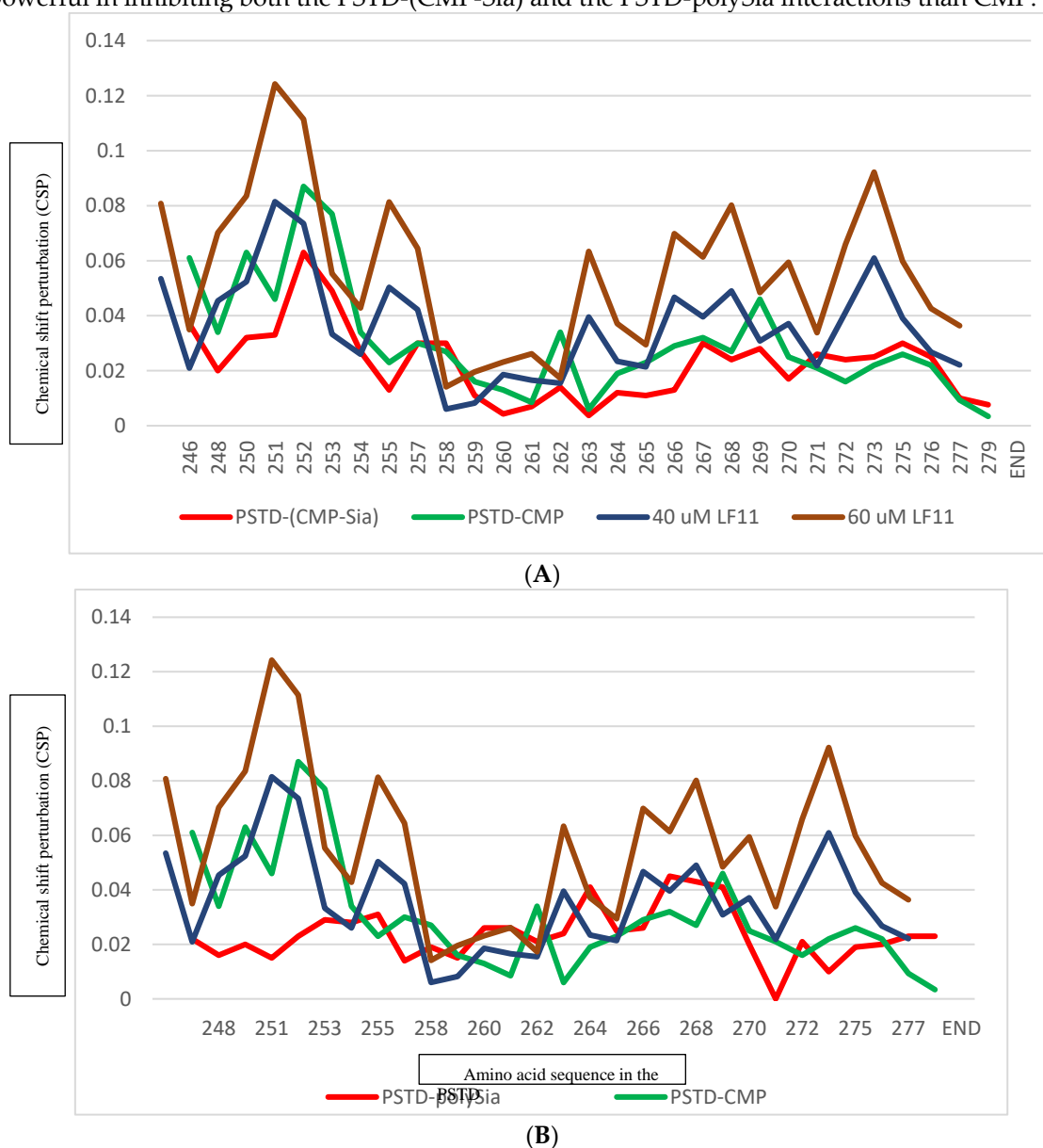


Figure 5. The Chemical shift perturbations (CSPs) of the PSTD when it interacted with 1mM CMP-Sia, 80 μ M CMP, and 40 μ M and 60 μ M LFcinB11, respectively (A); and the CSPs of the PSTD when it interacted with 0.1 mM PSA, 1mM CMP, and 40 μ M and 60 μ M LFcinB11, respectively (B).

The previous NMR studies indicated that heparin LMWH is an effective inhibitor of NCAM polysialylation. Twelve residues, N247, V251, R252, T253, S257, R265, Y267, W268, L269, V273, I275, and K276 in the PSTD were discovered to be the binding sites of the LMWH, and they were mainly located on the long α -helix of the PSTD, and the short 3-residue loop of the C-terminal PSTD [23]. The range of LMWH binding to the PSTD is almost same with that of the LF (Figure 6). As shown in Figure 6a and Table 2, the CSPs of the PSTD for the PSTD-LMWH (80 μ M) interaction are larger than that for the PSTD-(CMP-Sia) interaction, indicated the PSTD-(CMP-Sia) binding could be inhibited by 80 μ M LMWH. However, only take 40 μ M LF, both the PSTD-(CMP-Sia) interaction and the PSTD-polySia interaction could be inhibited (Figure 6b). In addition, as an inhibitor LFcinB11 may be more safety than LMWH. Because the intracerebral hemorrhage of patients was related to heparin intake [29].

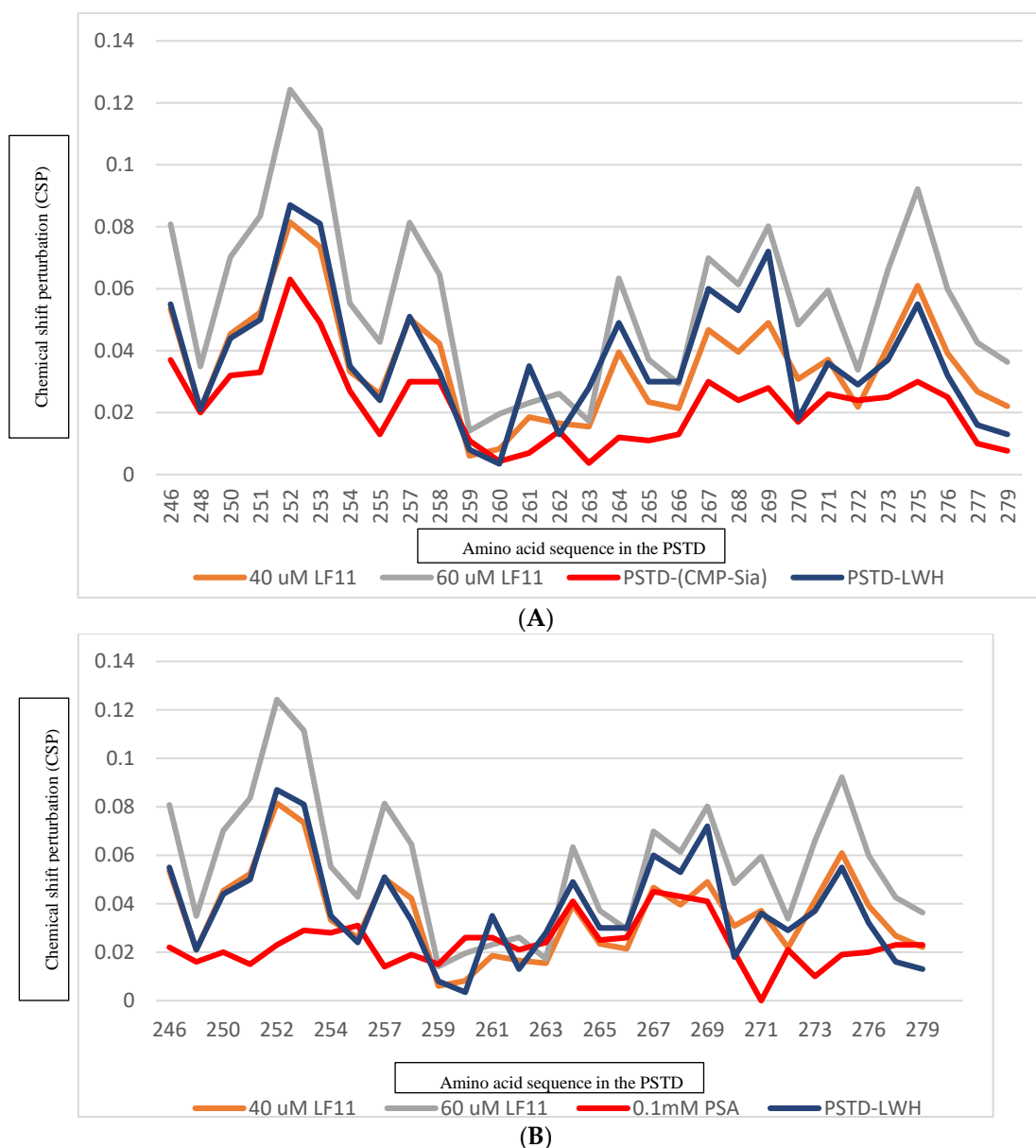


Figure 6. The Chemical shift perturbations (CSPs) of the PSTD when it interacted with 1mM CMP-Sia, 80 μ M heparin LMWH, and 40 μ M and 60 μ M LFcInB11, respectively (A); and the CSPs of the PSTD when it interacted with 0.1 mM PSA, 80 μ M heparin LWLH, and 40 μ M and 60 μ M LFcInB11, respectively (B).

LFcInB11 not only can interact with the PSTD to inhibit the interactions of the PSTD-(CMP-Sia) and the PSTD-polySia, but also can directly interact with polySia (Figure 4). This NMR result is consistent with the results using *in vitro* experiments [32–34], and proposed that the major contribution of the interaction between LF and polySia is from the N-terminal residues of LF, particularly in LFcInB11 domain.

4. Materials and Methods

4.1. Material Sources

The PSTD (246K-277R) should be a 32 amino acid sequence peptide from ST8Sia IV molecule. However, in order to obtain more accurate 3D structural information by NMR spectroscopy, one amino acid (245L) and two amino acids (278P and 279S) from ST8Sia IV sequence were added into the N- and C- terminals of PSTD, respectively [12–14,25,30]. Thus, a 35 amino acid sequence peptide sample containing PSTD was synthesized as follows:

245LKNKLVRTAYPSLRLIHAVRGYWLTKVPIKRPS279". In which, the PSTD sequence is labelled by underline. This intact peptide sample was chemically synthesized by automated solid-phase synthesis using the F-MOC-protection strategy and purified by HPLC (GenScript, NanJing, China). Its molecular weight was determined to be 4117.95 and its purity established to be 99.36%.

LFcinB11 peptide was purchased from BACHEM, amino sequence RRWQWRMKKLG, and relative molecular mass 1544.8. PolySia were purchased from Santa Cruz Biotechnology.

4.2. Circular Dichroism (CD) Spectroscopy

The concentrations of the 35 amino acid-PSTD peptide and LFcinB11 in 20 mM phosphate buffer (pH 6.7) with 25% tetrafluoroethylene (TFE) were 8.0 μ M and 400 μ M, respectively. The measured and recorded methods of CD spectra are the same as the previous articles [23,30].

4.3. NMR Sample Preparation

The 35 amino acid peptide containing the PSTD was prepared as described above in a 20 mM phosphate buffer containing 25% TFE. Chemical shifts were referenced with respect to 2-dimethyl-2-silapentane-5-sulfonic acid (DSS) used as the internal standard.

For both the 1-D and 2-D NMR experiments, the concentration of the PSTD peptide in the absence or the presence of LFcinB11 was 2.0 mM. The concentrations of LFcinB11 in the presence of the PSTD were all 20, 40, 60, and 80 μ M, respectively. For 2-D NMR experiments of the polySia-LBcinB11 interaction, the concentration of polySia and LFcinB11 are all 50 μ M.

All NMR samples were dissolved in 25% TFE (*v/v*), 10% D₂O (*v/v*), and 65% (*v/v*) 20 mM phosphate buffer (pH 6.7). Following this, 2-Dimethyl-2-silapentane-5-sulfonic acid (DSS) was added to all samples to serve as a reference standard.

4.4. NMR Spectroscopic Methods

NMR spectroscopy is a *powerful* tool for studying biomolecule-protein (DNA) or protein-ligand interactions [36–45]. All NMR spectra were recorded at 298 K using an Agilent DD2 800 MHz spectrometer equipped with a cold-probe in the NMR laboratory at the Guangxi Academy of Sciences. Water resonance was suppressed using pre-saturation. NOESY mixing times were set at 300 msec while the TOCSY experiments were recorded with mixing times of 80 msec [30,46]. All chemical shifts were referenced to the internal DSS signal set at 0.00 ppm for proton, and indirectly for carbon and nitrogen [23,30]. Data were typically apodized with a shifted sine bell window function and zero-filled to double the data points in F1, prior to being Fourier transformed. NMRPipe [23,30]. CcpNmr (www.ccpn.ac.uk/v2-software/analysis) was used for processing the data and spectral analysis. Spin system identification and sequential assignment of individual resonances were carried out using a combination of TOCSY and NOESY spectra, as previously described [23,30], and coupled with an analysis of ¹H-¹⁵N and ¹H-¹³C HSQC for overlapping resonances. In order to identify and characterize the specificity of the PSTD-ligand binding, the chemical shift perturbation (CSP) of each amino acid in the PSTD was calculated using the formula:

$$\text{CSP} = [(D_{\text{NH}}^2 + (D_{\text{N}}/5)^2)/2]^{1/2} \quad (1)$$

Where, D_{N} and D_{NH} represent the changes in ¹⁵N and ¹H chemical shifts, respectively, upon ligand binding [46].

5. Conclusion

Our results indicate that LFcin11 is a more powerful inhibitor than LMWF and CMP, and can be safely used. Furthermore, the bifunctional effects of LFcinB11 are proposed, i.e. LFcinB11 not only can inhibit the NCAM polysialylation through the PSTD-LFcinB11 interaction, but also inhibit the formation of neutrophil extracellular traps (NETs), a network of extracellular strings of DNA that bind pathogenic microbes [46–56]. Because the NETs role in promoting tumor metastasis formation

could be blocked by addition of LFcin B11 [57–62], a binfunctional effect of LFcinB11 has been proposed in this study. In the future studies, we will further study the molecular mechanism of the interaction between polySia and LFcinB11 to understand how does LFcin block tumor metastasis formation related to the formation of the NETs.

Author Contributions: The manuscript was written through contributions of all authors. All authors have given approval to the final version of the manuscript. Conceptualization, GP. Z and RB. H.; Methodology, B.L., JX.L. & XH. L; Validation, SM. L. & L.X.P.; Formal Analysis, GP. Z.; Investigation, B.L., SJ. L and GP.Z.; Writing – Original Draft Preparation, GP.Z.; Writing – Review & Editing, GP.Z.; Supervision, GP. Z & RB. H.; Project Administration, SM. L; Funding Acquisition, SM. L., B. L & GP.Z.

Funding Sources: This research was supported by National Natural Science Foundation of China (32060216) , Guangxi Science and Technology Base and Talent Project (GuiKe AA20297007, Nanning Scientific Research and Technology Development Project (20223038) , Guangxi Major science and technology Innovation base construction project (2022-36-Z06-01) , Central Guidance Fund for Local Scientific and Technological Development Project (Guike ZY23055011) .

Institutional Review Board Statement: Not applicable.

Informed Consent Statement: Not applicable.

Data Availability Statement: Not applicable.

Acknowledgements: The authors thank the 800 MHz NMR facility of Guangxi Academy of Sciences for the support in using NMR spectra acquirement.

Conflicts of Interest: The authors declare no conflict of interest.

Abbreviations

polySia	polysialic acid
Sia	mono-sialic acid
CMP-Sia	cytidine monophosphate-sialic acid
NCAMs	neural cell adhesion molecules
polySTs	polysialyltransferases (ST8Sia II (STX) & ST8Sia IV (PST)
PSTD	polysialyltransferase domain
LMWH	Low molecular weight heparin
CMP	cytidine monophosphate
LF	Lactoferrin
CSP	chemical shift perturbation

References

1. Lepers, A.H.; Petit, D.; Mollicone, R.; Delannoy, P.; Petit, J.M.; Oriol, R. Evolutionary history of the alpha2,8-sialyltransferase (ST8Sia) gene family: Tandem duplications in early deuterostomes explain most of the diversity found in the vertebrate ST8Sia genes. *Evolutionary Biology.*, **2008**, *8*, 258.
2. Jeanneau, C.; Chazalet, V.; Augé, C.; Soumpasis, D.M.; Harduin-Lepers, A.; Delannoy, P.; Imberty, A.; Breton, C. Structure- function analysis of the human sialyltransferase ST3Gal I: role of n-glycosylation and a novel conserved sialylmotif. *J. Biol. Chem.*, **2004**, *279*(14), 13461-13468. [<http://dx.doi.org/10.1074/jbc.M311764200>] [PMID: 14722111]
3. Sasaki, K.; Kurata, K.; Kojima, N.; Kurosawa, N.; Ohta, S.; Hanai, N.; Tsuji, S.; Nishi, T. Expression cloning of a GM3-specific al- pha-2,8-sialyltransferase (GD3 synthase). *J. Biol. Chem.*, **1994**, *269*(22), 15950-15956. [PMID: 8195250]
4. Nakayama, J.; Fukuda, M.N.; Hirabayashi, Y.; Kanamori, A.; Sasaki, K.; Nishi, T.; Fukuda, M. Expression cloning of a human GT3 synthase. GD3 AND GT3 are synthesized by a single enzyme. *J. Biol. Chem.*, **1996**, *271*(7), 3684-3691. [<http://dx.doi.org/10.1074/jbc.271.7.3684>] [PMID: 8631981]
5. Johnson, C.P.; Fujimoto, I.; Rutishauser, U.; Leckband, D.E. Direct evidence that neural cell adhesion molecule (NCAM) polysialyla- tion increases intermembrane repulsion and abrogates adhesion. *J. Biol. Chem.*, **2005**, *280*(1), 137-145. [<http://dx.doi.org/10.1074/jbc.M410216200>] [PMID: 15504723]

6. Seidenfaden, R.; Krauter, A.; Schertzinger, F.; Gerardy-Schahn, R.; Hildebrandt, H. Polysialic acid directs tumor cell growth by controlling heterophilic neural cell adhesion molecule interactions. *Mol. Cell. Biol.*, **2003**, *23*(16), 5908-5918. [<http://dx.doi.org/10.1128/MCB.23.16.5908-5918.2003>] [PMID: 12897159]
7. Eggers, K.; Werneburg, S.; Schertzinger, A.; Abeln, M.; Schiff, M.; Scharenberg, M.A.; Burkhardt, H.; Mühlenhoff, M.; Hildebrandt, H. Sialic acid controls NCAM signals at cell-cell contacts to regulate focal adhesion independent from FGF receptor activity. *J. Cell Sci.*, **2011**, *124*(Pt 19), 3279-3291.
8. Troy, F.A., II Polysialylation: from bacteria to brains. *Glycobiology*, **1992**, *2*(1), 5-23. [<http://dx.doi.org/10.1093/glycob/2.1.5>] [PMID: 1550990]
9. Petit, D.; Teppa, E.; Mir, A.M.; Vicogne, D.; Thisse, C.; Thisse, B.; Filloux, C.; Harduin-Lepers, A. Integrative view of α 2,3- sialyltransferases (ST3Gal) molecular and functional evolution in deuterostomes: significance of lineage-specific losses. *Mol. Biol. Evol.*, **2015**, *32*(4), 906-927.
10. Zhou, G.-P.; Liao, S.-M.; Chen, D.; Huang, R.-B., The Cooperative Effect between Polybasic Region (PBR) and Polysialyltransferase Domain (PSTD) within Tumor-Target Polysialyltransferase ST8Sia II. *Current Topics in Medicinal Chemistry* **2020**, *19*, (31), 2831-2841.
11. Huang, R. B.; Cheng, D.; Liao, S. M.; Lu, B.; Wang, Q. Y.; Xie, N. Z.; Troy, F. A.; Zhou, G. P., The Intrinsic Relationship Between Structure and Function of the Sialyltransferase ST8Sia Family Members. *Curr Top Med Chem*, **2017**, *17*, (21), 2359-2369.
12. Liao, S. M.; Lu, B.; Liu, X. H.; Lu, Z. L.; Liang, S. J.; Chen, D.; Troy, F. A.; Huang, R. B.; Zhou, G. P., Molecular Interactions of the Polysialyltransferase Domain (PSTD) in ST8Sia IV with CMP-Sialic Acid and Polysialic Acid Required for Polysialylation of the Neural Cell Adhesion Molecule Proteins: An NMR Study. *Int J Mol Sci*, **2020**, *21*, (5).
13. Liao, S. M.; Liu, X. H.; Peng, L. X.; Lu, B.; Huang, R. B.; Zhou, G. P., Molecular Mechanism of Inhibition of Polysialyltransferase Domain (PSTD) by Heparin. *Curr Top Med Chem*, **2021**, *21*, (13), 1113-1120.
14. Lu, B.; Liu, X. H.; Liao, S. M.; Lu, Z. L.; Chen, D.; Troy, F. A.; Huang, R. B.; Zhou, G. P., A Possible Modulation Mechanism of Intramolecular and Intermolecular Interactions for NCAM Polysialylation and Cell Migration. *Curr Top Med Chem*, **2019**, *19*, (25), 2271-2282.
15. Zhou, G. P., The Medicinal Chemistry of Structure-based Inhibitor/Drug Design: Current Progress and Future Prospective. *Curr Top Med Chem*, **2021**, *21*, (13), 1097-1098.
16. Nakata, D.; Zhang, L.; Troy, F. A., Molecular basis for polysialylation: A novel polybasic polysialyltransferase domain (PSTD) of 32 amino acids unique to the α 2,8-polysialyltransferases is essential for polysialylation. *Glycoconjugate Journal* **2006**, *23*, (5-6), 423-436.
17. Zhou, G. P.; Chou, K. C., Two Latest Hot Researches in Medicinal Chemistry. *Curr Top Med Chem* **2020**, *20*, (4), 264-265.
18. Zhou, G. P., The Latest Researches of Enzyme Inhibition and Multi-Target Drug Predictors in Medicinal Chemistry. *Med Chem* **2019**, *15*, (6), 572-573.
19. Guan, F.; Wang, X.; He, F. Promotion of Cell Migration by Neural Cell Adhesion Molecule (NCAM) Is Enhanced by PSA in a Polysialyltransferase-Specific Manner. *PLoS ONE* **2015**, *10*, e0124237. <https://doi.org/10.1371/journal.pone.0124237>.
20. Elkashef, S.M.; Allison, S.J.; Sadiq, M.; Basheer, H.A.; Morais, G.R.; Loadman, P.M.; Pors, K.; Falconer, R.A. Polysialic acid sustains cancer cell survival and migratory capacity in a hypoxic environment. *Sci. Rep.* **2016**, *6*, 33026. <https://doi.org/10.1038/srep33026>.
21. Al-Saraireh, Y.M.; Sutherland, M.; Springett, B.R.; Freiburger, F.; Morais, G.R.; Loadman, P.R.; Errington, R.J.; Smith, P.J.; Fukuda, M.; Gerardy-Schahn, R.; et al. Pharmacological inhibition of polysialyltransferase ST8SiaII modulates tumour cell migration. *PLoS ONE* **2013**, *8*, e73366.
22. Li, J.; Dai, G.; Cheng, Y.B.; Qi, X.; Geng, M.Y. Polysialylation promotes neural cell adhesion molecule-mediated cell migration in a fibroblast growth factor receptor-dependent manner, but independent of adhesion capability. *Glycobiology* **2011**, *21*, 1010-1018.
23. Peng, L.X.; Liu, X.H.; Lu, B.; Liao, S.M.; Zhou, F.; Huang, J.M.; Chen, D.; Troy, F.A.; Zhou, G.P.; Huang, R.B. The inhibition of polysialyltransferase st8siaiv through heparin binding to polysialyltransferase domain (PSTD). **2019**, *15*(5):486-495.
24. Zhou, G. P.; Huang, R. B., The Graphical Studies of the Major Molecular Interactions for Neural Cell Adhesion Molecule (NCAM) Polysialylation by Incorporating Wenxiang Diagram into NMR Spectroscopy. *Int J Mol Sci* **2022**, *23*, (23).

25. Zhou, G. P.; Chen, D.; Liao, S.; Huang, R. B., Recent Progresses in Studying Helix-Helix Interactions in Proteins by Incorporating the Wenxiang Diagram into the NMR Spectroscopy. *Curr Top Med Chem* **2016**, *16*, (6), 581-90.
26. Zhou, G. P., The disposition of the LZCC protein residues in wenxiang diagram provides new insights into the protein-protein interaction mechanism. *J Theor Biol* **2011**, *284*, (1), 142-8.
27. Chou, K.-C., The Significant and Profound Impacts of Chou's "wenxiang" Diagram. *Voice of the Publisher* **2020**, *06*, (03), 102-103.
28. Chou, K.-C.; Lin, W.-Z.; Xiao, X., Wenxiang: a web-server for drawing wenxiang diagrams. *Natural Science* **2011**, *03*, (10), 862-865.
29. Babikian, V.L., Kase, C.S., Pessin, M.S., Norrving, B., and Gorelick, P.B. Intracerebral hemorrhage in stroke patients anticoagulated with heparin. *Stroke*. **1989**, *20*(11):1500-3. doi: 10.1161/01.str.20.11.1500.
30. Lu, B.; Liao, S. M.; Liu, X. H.; Liang, S. J.; Huang, J.; Lin, M.; Meng, L.; Wang, Q. Y.; Huang, R. B.; Zhou, G. P., The NMR studies of CMP inhibition of polysialylation. *J Enzyme Inhib Med Chem* **2023**, *38*, (1), 2248411.
31. Kühnle, A., Veelken, R., Galuska, C.E., Saftenberger, M., Verleih, M., Schuppe, H.C., Rudlo, S., Kunz, C., and Galuska, S.P. Polysialic acid interacts with lactoferrin and supports its activity to inhibit the release of neutrophil extracellular traps. *Carbohydrate Polymer*, **2019**, 32-41.
32. Gifford J.L., Hunter H.N., and Vogel H.J. Lactoferricin: a lactoferrin-derived peptide with antimicrobial, antiviral, antitumor and immunological properties. *Cell. Mol. Life Sci.* **2005**, *62*(22): 2588-2598.
33. KANG, J.H., LEE, M.K., KIM, K.L., and HAHM, K.S. Structure-biological activity relationships of 11-residue highly basic peptide segment of bovine lactoferrin. *Int. J. Peptide Protein Res.* **48**, **1996**, 357-363.
34. Bellamy, W., Takase, M., Yamauchi, K., Wakabayashi, H., Kawase, K. & Tomita, M. *Biochim. Biophys. Acta*, **1992**, **1121**, 130-136.
35. Ortiz, A. I.; Reglero, A.; Rodriguez-Aparicio, L. B.; Luengo, J. M., In vitro synthesis of colominic acid by membrane-bound sialyltransferase of *Escherichia coli* K-235. Kinetic properties of this enzyme and inhibition by CMP and other cytidine nucleotides. *Eur J Biochem* **1989**, *178*, (3), 741-9.
36. Fu, Q.; Piai, A.; Chen, W.; Xia, K.; Chou, J. J., Structure determination protocol for transmembrane domain oligomers. *Nat Protoc* **2019**, *14*, (8), 2483-2520.
37. Schnell, J. R.; Zhou, G. P.; Zweckstetter, M.; Rigby, A. C.; Chou, J. J., Rapid and accurate structure determination of coiled-coil domains using NMR dipolar couplings: application to cGMP-dependent protein kinase Ialpha. *Protein Sci* **2005**, *14*, (9), 2421-8.
38. Sharma, A. K.; Zhou, G. P.; Kupferman, J.; Surks, H. K.; Christensen, E. N.; Chou, J. J.; Mendelsohn, M. E.; Rigby, A. C., Probing the interaction between the coiled coil leucine zipper of cGMP-dependent protein kinase Ialpha and the C terminus of the myosin binding subunit of the myosin light chain phosphatase. *J Biol Chem* **2008**, *283*, (47), 32860-9.
39. Berardi, M. J.; Shih, W. M.; Harrison, S. C.; Chou, J. J., Mitochondrial uncoupling protein 2 structure determined by NMR molecular fragment searching. *Nature* **2011**, *476*, (7358), 109-13.
40. OuYang, B.; Xie, S.; Berardi, M. J.; Zhao, X.; Dev, J.; Yu, W.; Sun, B.; Chou, J. J., Unusual architecture of the p7 channel from hepatitis C virus. *Nature* **2013**, *498*, (7455), 521-5.
41. Oxenoid, K.; Dong, Y.; Cao, C.; Cui, T.; Sancak, Y.; Markhard, A. L.; Grabarek, Z.; Kong, L.; Liu, Z.; Ouyang, B.; Cong, Y.; Mootha, V. K.; Chou, J. J., Architecture of the mitochondrial calcium uniporter. *Nature* **2016**, *533*, (7602), 269-73.
42. Chen, W.; OuYang, B.; Chou, J. J., Critical Effect of the Detergent:Protein Ratio on the Formation of the Hepatitis C Virus p7 Channel. *Biochemistry* **2019**, *58*, (37), 3834-3837.
43. Fu, Q.; Fu, T. M.; Cruz, A. C.; Sengupta, P.; Thomas, S. K.; Wang, S.; Siegel, R. M.; Wu, H.; Chou, J. J., Structural Basis and Functional Role of Intramembrane Trimerization of the Fas/CD95 Death Receptor. *Mol Cell* **2016**, *61*, (4), 602-613.
44. Joseph, P. R.; Poluri, K. M.; Sepuru, K. M.; Rajarathnam, K., Characterizing protein-glycosaminoglycan interactions using solution NMR spectroscopy. *Methods Mol Biol* **2015**, *1229*, 325-33.
45. Bjorndahl, T. C.; Zhou, G. P.; Liu, X.; Perez-Pineiro, R.; Semenchenko, V.; Saleem, F.; Acharya, S.; Bujold, A.; Sobsey, C. A.; Wishart, D. S., Detailed biophysical characterization of the acid-induced PrP(c) to PrP(beta) conversion process. *Biochemistry* **2011**, *50*, (7), 1162-73.
46. Vaynberg, J.; Qin, J., Weak protein-protein interactions as probed by NMR spectroscopy. *Trends Biotechnol* **2006**, *24*, (1), 22-7.

47. Yadav, R., Yoo, D.g., Rada, B. Michelle Kahlenberg, J., Bridges Jr, S.L., Oni, O., Huang, H., Stecenko, A., Rada, B. Systemic levels of anti-PAD4 autoantibodies correlate with airway obstruction in cystic fibrosis. *Journal of Cystic Fibrosis*, **2019**, 18, 636–645.
48. Brinkmann V, Reichard U, Goosmann C, Fauler B, Uhlemann Y, Weiss DS, et al. Neutrophil extracellular traps kill bacteria. *Science* **2004**;303(5663):1532–5.
49. Yoo DG, Winn M, Pang L, Moskowitz SM, Malech HL, Leto TL, et al. Release of cystic brosis airway in"ammatory markers from Pseudomonas aeruginosa-stimulated human neutrophils involves NADPH oxidase-dependent extracellular DNA trap for- mation. *J Immunol* **2014**;192(10):4728–38.
50. Yoo DG, Floyd M, Winn M, Moskowitz SM, Rada B. NET formation induced by Pseudomonas aeruginosa cystic !brosis isolates measured as release of myeloperoxidase-DNA and neutrophil elastase-DNA complexes. *Immunol Lett* **2014**;160(2):186–94.
51. Manzenreiter R, Kienberger F, Marcos V, Schilcher K, Krautgartner WD, Obermayer A, et al. Ultrastructural characterization of cystic fibrosis sputum using atomic force and scanning electron microscopy. *J Cyst Fibros* **2012**;11(2):84–92.
52. Papayannopoulos V, Staab D, Zychlinsky A. Neutrophil elastase enhances sputum solubilization in cystic !brosis patients receiving DNase therapy. *PLoS One* 2011;6 (12):e28526.
53. Li, P., Li, M., Lindberg, M.R., Kennett, M.J., Xiong N, Wang Y. PAD4 is essential for antibacterial innate immunity mediated by neutrophil extracellular traps. *J Exp Med*. **2010**, 207(9):1853–62.
54. Wang, ., Li, M, Stadler, S,, Correll, S,, Li, P., Wang, D., etal. Histone hypercitrullination mediates chromatin decondensation and neutrophil extracellular trap formation. *J Cell Biol*. **2009**,184(2):205–13.
55. Dwivedi N, Radic M. Citrullination of autoantigens implicates NETosis in the induction of autoimmunity. *Ann Rheum Dis*. **2014**,73(3):483–91.
56. Pang L, Hayes CP, Buac K, Yoo DG, Rada B. Pseudogout-associated in"ammatory calcium pyrophosphate dihydrate microcrystals induce formation of neutrophil extracellular traps. *J Immunol* **2013**,190(12):6488–500.
57. LewisHD,LiddleJ,CooteJE,AtkinsonSJ,BarkerMD,BaxBD,etal.InhibitionofPAD4 activity is sufficient to disrupt mouse and human NET formation. *Nat Chem Biol*, **2015**, 11(3):189–91.
58. Cao, X., Ren, Y., Lu, Q., Wang, K, Wu., Wang, Y., Zhang, Y., Cui, X., Yang, Z. and Chen, Z. Lactoferrin: A glycoprotein that plays an active role in human health. *Front. Nutr.* **2023**, 9:1018336. doi: 10.3389/fnut.2022.1018336.
59. Gibbons J, Kanwar R, Kanwar J. Lactoferrin and cancer in dierent cancer models. *Front Biosci*. **2011**, 3:1080. doi: 10.2741/212.
60. Elzoghby A, Abdelmoneem M, Hassanin I, Abd Elwakil M, Elnaggar M, Mokhtar S, et al. Lactoferrin, a multi-functional glycoprotein: active therapeutic, drug nanocarrier & targeting ligand. *Biomaterials*. **2020**, 263:120355. doi: 10. 1016/j.biomaterials.2020.120355.
61. Morgenthau A, Pogoutse A, Adamiak P, Moraes T, Schryvers A. Bacterial receptors for host transferrin and lactoferrin: molecular mechanisms and role in host-microbe interactions. *Future Microbiol.* (2013) 8:1575–85. doi: 10.2217/fmb. 13.125.
62. Kell D, Heyden E, Pretorius E. The biology of lactoferrin, an iron-binding protein that can help defend against viruses and bacteria. *Front Immunol*. **2020**,11:1221. doi: 10.3389/fimmu.2020.01221.

Disclaimer/Publisher's Note: The statements, opinions and data contained in all publications are solely those of the individual author(s) and contributor(s) and not of MDPI and/or the editor(s). MDPI and/or the editor(s) disclaim responsibility for any injury to people or property resulting from any ideas, methods, instructions or products referred to in the content.